Chemical Engineering Science 234 (2021) 116456

Contents lists available at ScienceDirect

Chemical Engineering Science

journal homepage: www.elsevier.com/locate/ces

Diffusion-based modeling of film growth of hydrates on gas-liquid interfaces

Aritra Kar [a], Awan Bhati [a], Palash V. Acharya [a], Ashish Mhadeshwar [b], Pradeep Venkataraman [c], Timothy A. Barckholtz [b], Vaibhav Bahadur [a,*]

[a] Walker Department of Mechanical Engineering, The University of Texas at Austin, Austin, TX, United States
[b] ExxonMobil Research and Engineering, Annandale, NJ, United States
[c] ExxonMobil Upstream Research Company, Houston, TX, United States

ARTICLE INFO

Article history:
Received 1 September 2020
Received in revised form 2 December 2020
Accepted 11 January 2021
Available online 23 January 2021

Keywords:
Hydrates
Film growth
Diffusion
Kinetics
Heat transfer
Subcooling

ABSTRACT

Formation of gas hydrates occurs in three stages: nucleation, film growth, and bulk growth. As per past literature, the rate of film growth (on gas-liquid interface) depends on heat transfer from the vicinity of the film front to the surrounding medium. We present analyses to show that heat transfer is not a significant factor in film growth, as previously believed. We then present an alternative theory for film growth, which considers film growth as gas diffusion limited. We note that gas diffusion through hydrates is a limiting phenomena for bulk growth; we presently show that diffusion from the gas phase is the limiting phenomena for film growth as well. This fundamentals-based analytical model does not need the significant assumptions invoked in previous studies and relies on only one fitting parameter. Importantly, the model shows excellent agreement with experimental results on film growth of hydrates from pure gases and mixtures of gases.

1. Introduction

Gas hydrates are ice-like crystalline solids which form under high pressure and low temperature conditions from gas and water. Structurally, gas hydrates consist of gas molecules trapped in cages of water molecules which are stabilized by hydrogen bonds (Makogon, 1997; Sloan and Koh, 2008). Gas hydrates have promising applications in methane (CH_4) transport, desalination, and carbon dioxide (CO_2) sequestration (Koh et al., 2011). Although the thermodynamics of hydrate formation is well-understood, modeling hydrate growth kinetics is challenging owing to limitations in our current understanding of nucleation, gas diffusion, kinetics, and heat transfer. There exist multiple reviews on detailed mechanisms associated with the nucleation and growth of gas hydrates (Khurana et al., 2017; Ribeiro and Lage, 2008; Yin et al., 2018).

Hydrate nucleation generally occurs at the gas-liquid interface near the three-phase contact line (Acharya et al., 2020; Khurana et al., 2017). The first "crystal" of nucleated hydrate grows on the surface of the gas-liquid interface near the high gas concentration region (Daniel-david et al., 2015; Li et al., 2014; Morrissy et al., 2017; Wu et al., 2013). This phase of hydrate growth is referred to as film growth (Sun et al., 2010; Sugaya and Mori, 1996). The reported initial thickness of hydrate films is generally less than 10 μm (Davies et al., 2010; Taylor et al., 2007). After the hydrate film forms at the gas-liquid interface, the gas phase is physically separated from the liquid phase, and hydrates grow towards both the liquid and gas phases. Film formation at the gas-water interface has also been observed during hydrate formation in porous media (Lei et al., 2019). Multiple articles in the last two decades claim that film growth is controlled by the rate of heat transfer (to remove the latent heat associated with hydrate formation) from the hydrate film to the surrounding medium (Liu et al., 2018; Mochizuki and Mori, 2017, 2006; Mori, 2001; Peng et al., 2007; Sun et al., 2010; Uchida et al., 1999).

In this work, *we present an alternative model for film growth, which does not involve heat transfer considerations*. We present fundamental reasons and detailed analyses to explain why heat transfer will not be a limiting factor during film growth of hydrates. The principal reason is the short time duration (less than a minute (Freer et al., 2001)) over which film growth happens. Water has a very high thermal effusivity (1500 $J/s^{1/2}m^2K$), which is a measure of its ability to absorb heat in a transient process. Therefore, water temperature will not increase significantly over the short time interval for film growth. This assertion is directly validated by experiments which report that an appreciable temperature rise

* Corresponding author.
E-mail address: vb@austin.utexas.edu (V. Bahadur).

https://doi.org/10.1016/j.ces.2021.116456
0009-2509/

occurs over several minutes (Corak et al., 2011; Kumar et al., 2016). We also present 1D and 2D transient heat diffusion scaling analysis during film growth to support our arguments. Subsequently, we present a diffusion-based analytical model to predict film growth of hydrates. *Importantly, our model has excellent agreement with multiple experimental datasets from literature, which shows that film growth kinetics is well-explained by fundamental mass transfer considerations.*

In the next section, we briefly review existing models for film growth and highlight their limitations. We then outline a diffusion-based modeling framework for film growth of hydrates from pure gases and gas mixtures. We would like to highlight the lack of empiricism and assumptions in our model, which is based on fundamental considerations, and consists of only one fitting parameter.

2. Review of existing models to predict film growth

Uchida et al. (1999) modeled the velocity of film front propagation during film growth of CO_2 hydrates. This involved a steady state balance between the rate of latent heat removal as the film grows and the rate of heat dissipation into the surrounding water. The model predicted the film growth velocity being proportional to the subcooling. Experimental data was linearly regressed with film thickness being a fitting parameter. However, there was significant deviation between the experimental data and theoretical predictions. Freer et al. (2001) developed a transient formulation similar to the classical Stephan's problem, which is used to model ice growth in supercooled water. This formulation predicted a growth rate which decreases with time and differs from the constant film growth rate observed in experiments (Freer et al., 2001; Kitamura and Mori, 2013). The experimental data was subsequently fitted using a correlation involving three fitting parameters, which accounted for the convection and rate kinetics.

Mori (2001) improved on Uchida et al. (1999)'s model by accounting for convection in the surrounding medium. Here, the film front velocity was proportional to the 3/2 power of subcooling. This model had a better match with experimental data (Mori, 2001). Mori's (2001) model was based on the assumption that as the film propagates, there is a relative velocity between the film and the stagnant surrounding which leads to forced convective heat transfer. However, film growth is the nucleation of new hydrate particles at the film front; the rest of the film does not have a relative velocity with respect to the surroundings. Mochizuki and Mori (2006) improved on Freer et al. (2001)'s model by considering a formulation based on 2D heat conduction. However, as with the limitations of Freer et. al.'s (2001) model, the velocity of the film front decayed with time, whereas it is observed to be constant in experiments.

Peng et al. (2007) proposed that the film thickness is inversely proportional to subcooling. This was an empirical observation; nevertheless, incorporating this relation into Mori's convection-based model (Mori, 2001) yielded the film front velocity to be proportional to the 5/2 power of subcooling. This model showed a good match with their in-house experiments (Peng et al., 2007). The assumption of film thickness being inversely proportional to subcooling was experimentally validated to a certain extent by Li-Li et al. (2013). However, it is noted that experimental measurements of film thickness were based only on the liquid side of the gas-liquid boundary because the thickness on the gas side could not be captured using their experimental setup (hydrate films grow on both sides of the gas-liquid interface).

Saito et al. (2010) and Kishimoto and Ohmura (2012) formulated models based on gas solubility in water as the driving force for film growth. Their model was generalized by Mochizuki and Mori (Mochizuki and Mori, 2017) who coupled the solubility-based driving force with heat transfer from the hydrate film. Their model concluded that the solubility-based driving force plays a much more significant role in film growth. However they did not report the match of simulations with experiment data. Liu et al. (Liu et al., 2018; Mori, 2001) replaced the forced convection approach of Mori (2001) with natural convection and obtained the film growth rate as a function of subcooling. Their model utilized the empirical relation originally proposed by Peng et al. (2007) that film thickness is inversely proportional to subcooling.

In addition to heat transfer-based models, attempts have been made to model film growth via a reaction-based formulation. A driving force of $\Delta g/RT$ was proposed by Sun et al. (2007) based on a hydrate formation reaction, which fitted well with experimental data. However, this model used two fitting parameters. The second fitting parameter accompanied the driving force, $\Delta g/RT$, and was intended to account for corrections due to the complexities associated with hydrate formation. Daniel-david et al. (2015) also reported a good fit of their experimental data with the reaction-based formulation.

In summary, there have been multiple attempts to model film growth of hydrates. A majority of approaches include analysis of heat transfer. These models involve significant assumptions (thickness of film, shape of film front) and empiricism, utilization of multiple fitting parameters (in some models). Furthermore, most modeling approaches have been benchmarked using limited experimental data. In contrast, we present a fundamentals-based analytical model (with only one fitting parameter) to predict film growth, which is validated more extensively than previous models.

3. Analysis of heat transfer during film growth of hydrates

Mass transfer and heat diffusion considerations are jointly analyzed to develop scaling arguments to provide details on aspects that would be relevant under heat transfer-limited film growth. We show that the temperature rise (ΔT) in the vicinity of the growing hydrate film is negligible. We show that $\Delta T << \Delta T_{sub}$ (subcooling), which is contrary to the assumptions made in literature (Liu et al., 2018; Mori, 2001; Peng et al., 2007; Uchida et al., 1999). Essentially, the heat dissipated by hydrate formation is primarily absorbed by water due to its significantly higher thermal effusivity (1500 $J/s^{1/2}m^2K$) as compared to gas (~6 $J/s^{1/2}$ m^2 K) (Nellis and Klein, 2009). To further illustrate, we analyze film growth of CH_4 hydrates at 274 K. Eqs. (2.7)–(2.11) are utilized to obtain the mass transfer rate and hence the scales of exothermic heat generation (which needs to be dissipated) associated with hydrate formation. The heat dissipation scale is formulated based on 1D transient heat absorption by the water medium. It is noted that the dimensionless number is of similar form as the Prater number, used in heterogeneous catalysis, except that the heat dissipation term is considered transient (Davies and Davies, 2003).

The scaling of the heat generated to the heat dissipated at the hydrate film front can be expressed as:

$$\frac{\text{Heat generated}}{\text{Heat dissipated}} = \frac{\frac{kA_f P_{eq}\beta\Delta T_{sub}\Delta H}{RT}}{\frac{eA_{int}\Delta T}{\sqrt{t}}} = \frac{k\delta P_{eq}\varsigma\Delta H\Delta T_{sub}\sqrt{t}}{eRTL\Delta T} \sim 1 \qquad (1.1)$$

where e is the effusivity of water, L is a length scale of the reactor, ΔH is the heat of the hydrate formation, δ is the initial film thickness, ΔT is the rise in temperature near the growing hydrate film, k is the mass transfer coefficient, R is the universal gas constant, T is the temperature, and ΔT_{sub} is the subcooling. P_{eq} and ζ are equilibrium pressure and a growth parameter respectively (defined later in Eq. (1.2)) and calculated at the temperature T). Values of all the parameters used in this estimation are detailed in the supplementary information.

The temperature rise in the vicinity of hydrate crystals can be obtained from the scaling argument developed in Eq. (1.1). The heat generated due to hydrate formation has to equal the heat dissipated. An appropriate scale for the temperature rise near the hydrate film front is therefore:

$$\frac{\Delta T}{\Delta T_{sub}} \sim \frac{k\delta P_{eq}\varsigma\Delta H\sqrt{t}}{eRTL} \tag{1.2}$$

Film growth occurs over a period of a few seconds (<1 min), which results in $\frac{\Delta T}{\Delta T_{sub}} <\sim 0.02$. The rise in temperature of water is thus, significantly lower than the subcooling for short time scales. This clearly implies that film growth will occur at temperatures very close to the existing experimental temperatures instead of the equilibrium temperature of hydrate formation. The time scale, τ corresponding to a significant temperature rise ($\Delta T \sim \Delta T_{sub}$) can be estimated as:

$$\tau \sim \left(\frac{eRTL}{k\delta P_{eq}\varsigma\Delta H}\right)^2 \tag{1.3}$$

The above equations yields a time scale of 35 h, showing that heat dissipation at the film front is much faster and a local steady state is not justified during film growth. However, it is noted that magnitude of these time scales has limited relevance in hydrate formation. After the initial hydrate film is formed on the interface (physically separating the two phases), it will thicken on both sides of the interface, which will change the time scales. Nevertheless, our analysis shows that considerations of a steady-state temperature at the hydrate film front (Liu et al., 2018; Mori, 2001; Peng et al., 2007; Uchida et al., 1999) are not justified.

The above 1D analysis assumed that any heat generated at the film front is dissipated through the entire gas-water interface, which is a simplification. We also present a 2D scaling analysis wherein heat is dissipated from the hydrate film front through propagation of cylindrical-shaped heat waves. Details of the derivation are provided in the supplementary material. It is noted that for a 1D analysis, the propagation of heat wave is flat and vertically downward. Due to the cylindrical geometry in the 2D scaling analysis, the temperature difference ratio is time-independent, because the rate of heat absorption by water becomes constant. The temperature rise near the hydrate film can be expressed as:

$$\frac{\Delta T}{\Delta T_{sub}} \sim \frac{k\delta P_{eq}\varsigma\Delta H}{\lambda RT} \tag{1.4}$$

All parameters in the above equation were defined earlier; λ is the thermal conductivity of water. A value of $\frac{\Delta T}{\Delta T_{sub}} <\sim 0.07$ is obtained for film growth of CH_4 hydrates at 274 K. This again shows that the rise in temperature is negligible as compared to the subcooling. It is noted that the 2D model does not capture the transient variation in temperatures, unlike the 1D model. However, the consideration of the cylindrical heat dissipation area in the 2D model is more realistic than the area used in the 1D model. Taken together, *these analyses clearly highlight the non-relevance of heat transfer as an influencing parameter for film growth.*

4. Formulation of a diffusion-based model for film growth

Fig. 1 is a schematic showing a hydrate film at the interface of gas and water; we use a sharp interface-based model. While the transport of gas molecules to the hydrate film front occurs from both sides of the interface, it is dominated by the gas-side of the interface. This is justified due to the lower concentrations of gas in water and the lower mass transfer coeffcients of gas on the liquid-side of the interface. Similarly, transport of water molecules needed to sustain hydrate growth can occur from both sides of the interface, but is dominated by the water side. Our model considers the transport of gas molecules to be the rate-limiting step since the concentration of water molecules is much larger than that of gas. More explanations on gas and water transport and related concentrations are provided in the supplementary material.

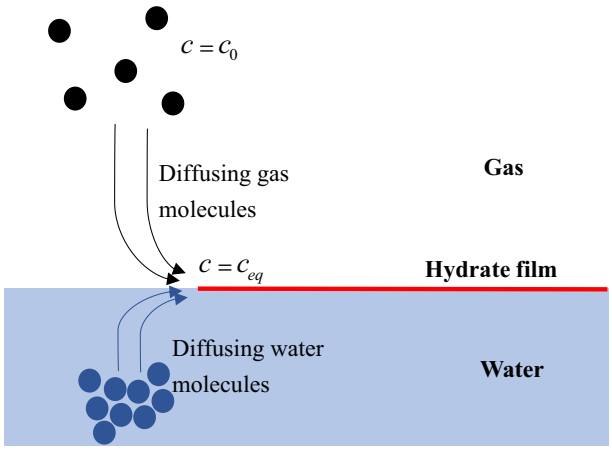

Fig. 1. Schematic showing a hydrate film growing at the gas-water interface.

We adopt a concentration-based formulation of a form similar to that proposed by Herri et al. (1999) and adopted by others (Hashemi et al., 2007; Herri et al., 1999; Turner et al., 2009), which considers the rate of hydrate crystal growth as diffusion-limited gas transport (Fig. 1). Hydrate crystal growth is a competition between the rate of diffusion of the gas to the hydrate crystals and gas adsorption into the cages. We note that, it is widely believed that gas diffusion to the vicinity of the hydrate crystals is the rate limiting step in reaction models for bulk hydrate growth (Hashemi et al., 2007; Herri et al., 1999; Turner et al., 2009). The rate of hydrate formation then takes the form:

$$r = kA_f(c - c_{eq}) \tag{2.1}$$

where r is the rate of hydrate formation, A_f is the interfacial area of the hydrate film front, c is the gas concentration in the gas phase, k is the mass transfer coefficient in the vicinity of the film front and c_{eq} is the equilibrium gas concentration. When pressure is at equilibrium conditions, i.e. $c \rightarrow c_{eq}$, the rate approaches zero. It should be noted that the equilibrium conditions are defined in the vicinity of the crystal and the equilibrium concentration is different from the bulk concentration of gas in water. The driving force for growth has also been related in terms of fugacity difference, $f - f_{eq}$, by Englezos et al. (1987). The gas concentration is defined in Eq. (2.2) using the ideal gas law and compressibility factors, which are calculated using the Peng-Robinson equation of state (Melhem et al., 1989). Z, P, R and T represent the compressibility factor, pressure, gas constant and experimental temperature, respectively.

$$c = \frac{P}{ZRT}, \quad c_{eq} = \frac{P_{eq}}{Z_{eq}RT}$$
$$Z = Z(P,T), \quad Z_{eq} = Z_{eq}(P_{eq},T) \tag{2.2}$$

We note that a similar concentration-based driving force of $c - c_{eq}$ was also obtained by Vlasov (2013) by considering first-order reversible reaction kinetics of hydrate formation, with the factor k being interpreted as the kinetic rate constant of the reaction. The idea of reaction-limited driving force was also proposed by Dashti et al. (2019) for modelling bulk hydrate growth. It is noted that bulk hydrate growth is usually limited by diffusion through hydrate layers, represented by concentration profiles akin to Fick's law (Buanes et al., 2006; Fu et al., 2018; Turner et al., 2009). Hence, such diffusion-based models are not uncommon in

studies of kinetics of bulk growth of hydrates. However, a diffusion-based formulation to capture film growth of hydrates has not been proposed in the available literature.

Substituting Eq. (2.2) into (2.1), we obtain:

$$r = kA_f\left(\frac{P}{ZRT} - \frac{P_{eq}}{Z_{eq}RT}\right) \approx \frac{\Delta P}{ZRT} \tag{2.3}$$

where ΔP is the overstep in pressure required for hydrate formation (higher pressure overstep leads to faster hydrate formation). Film growth is generally expressed in terms of subcooling ΔT_{sub}. We convert Eq. (2.3) in terms of temperature by adopting a form of the Antoine equation (or the Clausius Clapeyon equation) which describes the hydrate equilibrium conditions for pure gas hydrates. The thermodynamics of the Antoine equation yields:

$$\frac{d(\ln P)}{d\left(\frac{1}{T}\right)} = -A,\ \ \ln P = -\frac{A}{T} + B \tag{2.4}$$

P and T are pressure and temperature, respectively, under equilibrium conditions; A and B are constants. Experimentally obtained hydrate equilibrium curves can be fitted to obtain the constants A and B. The supplementary material shows linear regression of the equilibrium curve to obtain the constants A and B for CH_4 and CO_2 hydrates, as per the method outlined in Sloan and Koh (2008).

The applied pressure P determines the equilibrium temperature of formation of hydrates, T_{eq}. However, P_{eq} is the equilibrium pressure of formation at the experimental temperature, T. Since $P > P_{eq}$, and the equilibrium curve of hydrates has an upward slope ($\frac{dP}{dT} > 0$), we always have $T_{eq} > T$. The difference $\Delta T_{sub} = T_{eq} - T$ is the subcooling. A higher value of pressure overstep ΔP results in a higher value of subcooling (they are equivalent in terms of driving force for hydrate formation). This leads to:

$$\begin{aligned} \ln P &= -\tfrac{A}{T_{eq}} + B \\ \ln P_{eq} &= -\tfrac{A}{T} + B \end{aligned} \tag{2.5}$$

Next, we transform Eq. (2.3) in terms of subcooling using Eq. (2.5) as:

$$r = kA_f\left(\frac{\exp\left(-\frac{A}{T_{eq}} + B\right)}{ZRT} - \frac{\exp\left(-\frac{A}{T} + B\right)}{Z_{eq}RT}\right) \tag{2.6}$$

Eq. (2.6) can be simplified to express the rate in terms of ΔT_{sub} as:

$$r = \frac{kA_f \exp\left(-\frac{A}{T} + B\right)}{RT}\left(\frac{\exp\left(A\frac{\Delta T_{sub}}{TT_{eq}}\right)}{Z} - \frac{1}{Z_{eq}}\right) \tag{2.7}$$

Next, with the assumption of a thin film with frontal area A_f growing on the gas-water interface at a velocity $v_f(m/s)$, the rate can be related to hydrate properties as:

$$r = \frac{v_f A_f \rho}{M} \tag{2.8}$$

where ρ and M are the density and molecular weight of the hydrate, respectively. It is noted that no assumptions are made about the shape of the film front, as is the practice in previous models (Liu et al., 2018; Mochizuki and Mori, 2017, 2006; Mori, 2001; Uchida et al., 1999). From Eqs. (2.7) and (2.8), the velocity of film growth is:

$$v_f = \frac{kM}{\rho}\frac{\exp\left(-\frac{A}{T} + B\right)}{RT}\left(\frac{\exp\left(A\frac{\Delta T_{sub}}{TT_{eq}}\right)}{Z} - \frac{1}{Z_{eq}}\right) \tag{2.9}$$

It is noted that the velocity obtained in Eq. (2.9) is not directly related to the initial thickness of hydrate films, unlike other models in literature (Liu et al., 2018; Mochizuki and Mori, 2017; Mori, 2001; Peng et al., 2007; Uchida et al., 1999).

Nevertheless, we believe that the effective mass transfer coefficient k would not depend very significantly on the hydrodynamic conditions existing near film front. Hydrodynamic perturbations near the film front occurs due to the density differences between the forming hydrate and the surrounding fluid phases (gas and water). Such hydrodynamic perturbations will be affected by the shape of the hydrate film front, initial thickness of the hydrate films, curvature of the gas-water interface and stirring of the liquid phase. These effects on the mass transfer coefficient cannot be effectively captured through the sharp interface-based modelling adopted in this study, as it defines an overall coefficient k. Such effects are also discussed later in this manuscript, and in the supplementary information.

Further simplifications to the above model are possible, which enable useful insights. Since $\Delta T_{sub} \ll T$ (absolute temperature), the following approximations are valid:

$$\begin{aligned} \frac{1}{TT_{eq}} = \frac{1}{T(T+\Delta T_{sub})} = \frac{1}{T^2\left(1+\frac{\Delta T_{sub}}{T}\right)} \approx \frac{1}{T^2} \\ Z \approx Z_{eq} \end{aligned} \tag{2.10}$$

Eq. (2.9) can then be simplified as:

$$\begin{aligned} v_f &= \alpha(exp(\varsigma\Delta T_{sub}) - 1) \\ \alpha &= \frac{kM}{\rho}\frac{exp\left(-\frac{A}{T} + B\right)}{ZRT},\ \ \varsigma = \frac{A}{T^2} \end{aligned} \tag{2.11}$$

For a constant experimental temperature, α and ς will be constants. Eq. (2.11) can be expanded using a Taylor series (Eq. (2.12)) to result in the power law form of subcooling, which has been proposed previously by multiple authors (Liu et al., 2018; Mori, 2001; Peng et al., 2007; Uchida et al., 1999). Since typical subcooling values are small (between 2 and 12 K) and $\varsigma < 1$, lower order terms in the power series dominate, and the velocity of film growth can be expressed in terms of ΔT_{sub}^n, as:

$$v_f = \alpha\left(\varsigma\Delta T_{sub} + \frac{\varsigma^2}{2}\Delta T_{sub}^2 + \frac{\varsigma^3}{6}\Delta T_{sub}^3 + \frac{\varsigma^4}{24}\Delta T_{sub}^4 + ...\right) \tag{2.12}$$

Typically, the magnitude of the first four-five terms is significant and the series converges quickly. The convergence for CO_2 hydrates is shown numerically in the supplementary information. All of this explains how values of n ranging from 1.5 to 2.5 in ΔT_{sub}^n often accurately model experimental data (Daniel-david et al., 2015; Liu et al., 2018; Mori, 2001; Peng et al., 2007).

5. Results

5.1. Hydrate film formation from pure gases

Fig. 2a–c show the comparison of the predictions of the present model (Eq. (2.9)) with experimental measurements of hydrate film growth for pure gases. Experimental data from three past studies is available: (i) CH_4 hydrates from Peng et al. (2007), shown in Fig. 2a, (ii) CO_2 hydrates from Peng et al. (2007), shown in Fig. 2b, and (iii) CH_4 hydrates from Freer et al. (2001), shown in Fig. 2c. For all three cases, the film growth rate increases with subcooling due to the higher driving force for hydrate formation. It is seen that the presently developed model matches experimental data very well, across a range of temperatures and subcooling. The model utilizes one fitting parameter which combines mass transfer coefficient and hydrate properties into one overall growth rate constant K = kM/ρ in Eq. (2.9). As we have presently shown, our analytical formulation provides an exponential-like function for the film velocity as shown in Eq. (2.11). It should be noted that the theoretical fit is quite sensitive to the parameter ς which is an intrinsic parameter, and depends on gas hydrate properties.

This model does not consider variations in the density of hydrates and water with subcooling; this is reasonable because

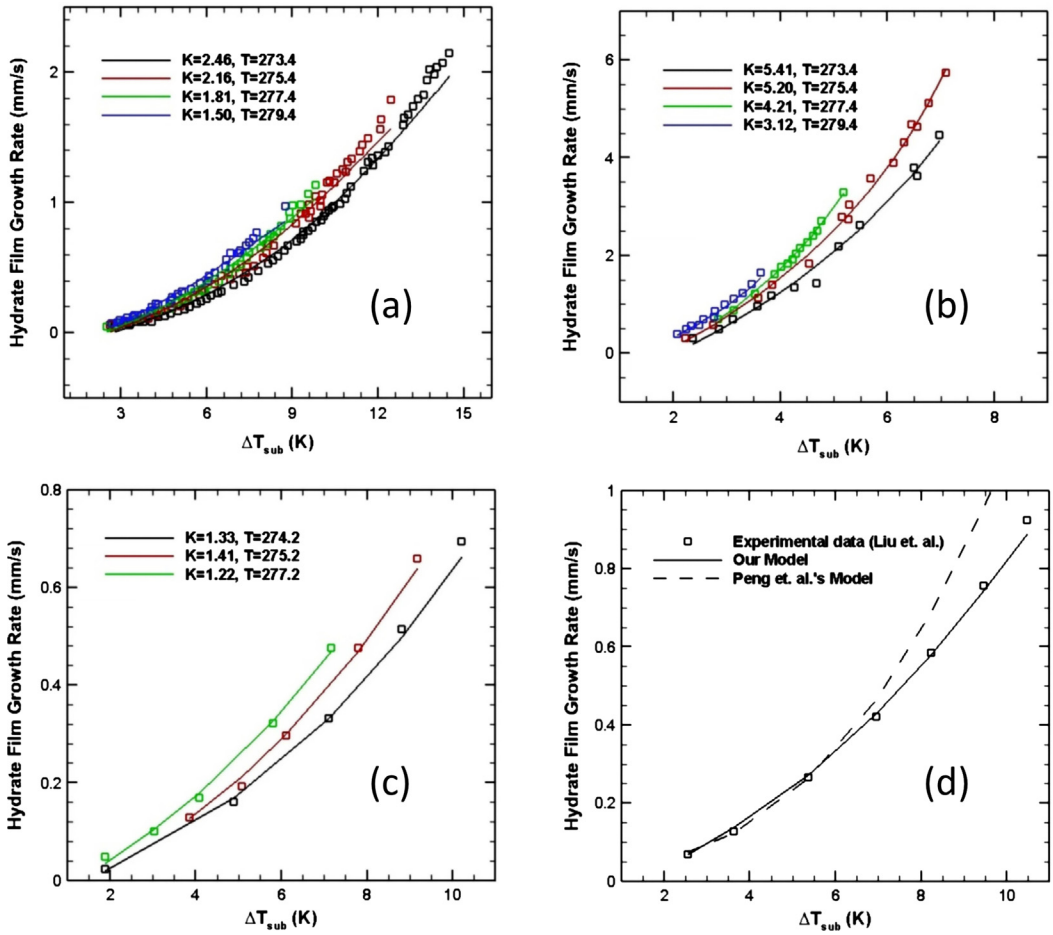

Fig. 2. Comparison of predictions of present model (equation) with experimentally measured growth rate of hydrate films for (a) CH_4 hydrates (Peng et al., 2007) (b) CO_2 hydrates (Peng et al., 2007), and (c) CH_4 hydrates (Freer et al., 2001). The plots compare theoretical predictions (curves) to experimental data (squares). (d) Comparison of the present model and the model by Peng et al. (2007) with the experimental data from Liu et al. (2018). K is the fitting parameter defined with units of 10^{-4} m^4/mol sec for CH_4 hydrates and 10^{-3} m^4/mol sec for CO_2 hydrates. All temperatures are in Kelvin. All R^2 values are greater than 0.98.

densities are not a strong function of pressure. The overall growth rate constant K is only considered as a function of temperature in the present model. However, it is noted that K also depends on the hydrodynamic perturbations near the film front as discussed before through its dependence on the mass transfer coefficient. We obtain K for CH_4 hydrates from Peng et al. (2007). This is in the range 1.5–2.5 $\times$ 10^{-4} m^4/mol sec, whereas K calculated from the data of Freer et al. (2001) ranges between 1.2 and 1.4 $\times$ 10^{-4} m^4/mol sec; these numbers are similar in magnitude. Such variations in mass transfer coeffcients across different experimental setups can be attributed to the variation in hydrodynamic conditions near the film front. As an illustration, Peng et al. (2007) investigated film growth on gas bubbles surrounded by water, whereas Freer et al. (2001)'s setup was a bulk gas-water system with a near-flat interface. Film growth variations due to reactor designs have also been reported in literature which might also contribute to such differences (Taylor et al., 2007; Wu et al., 2013). The model does capture such small variations in the overall growth rate constant K from CH_4 hydrates data in Fig. 2(a) and (c). For comparison, the value of K for CO_2 hydrates from Peng et al. (2007), is almost an order higher and is between 3.1 and 5.4 $\times$ 10^{-3} m^4/mol sec. It is instructive to compare the predictions of our model with previously developed models. One comparison is provided in Fig. 2d, which compares the predictions of the present model with those of Peng et al.'s (2007) model. It is noted that Peng et al.'s (2007) model is widely used, and was validated using the data from Liu et al. (2018). Fig. 2d shows that the present model has a better fit with the experimental data as compared to Peng et al.'s (2007) model, which was based on heat transfer-limited film growth. It is noted that Liu et al. (2018) also concluded that their experimental data was not well represented by Peng et al.'s (2007) model. In summary, our model validates multiple datasets from literature, which highlights the generality and utility of our theory.

5.2. Hydrate film formation from gas mixtures

We show that the predictions of our model formulation also match very well with experimental measurements of hydrate film growth from gas mixtures. The equilibrium curve for a mixture of gases is generally not a superimposition of the equilibrium curves of individual components in the mixture. It is also difficult to define mixture equilibrium curves using the Clausius-Clapeyron equation. Hence, we utilize the following correlation developed by Bahadori and Vuthaluru (Bahadori and Vuthaluru, 2009) to define the equilibrium curve for a mixture of hydrates:

$$\ln P = B + \frac{A}{T} + \frac{C}{T^2} + \frac{D}{T^3} \tag{2.13}$$

The constants A, B, C, and D in Eq. (2.13) depend on the overall molecular weight of the mixture (Bahadori and Vuthaluru, 2009). The compressibility factors for the mixture of gases are calculated

using the modified Peng-Robinson equation of state developed by Melhem et al. (Melhem et al., 1989). The binary interaction parameter for CH_4 and ethylene (C_2H_4) is assumed to be zero when calculating the compressibility factors (Melhem et al., 1989), because strong interactions between these components are not expected. Presently, we incorporate the equilibrium curve correlation and the compressibility factors in Eqs. (2.1) and (2.2) to conduct a simulation and obtain theoretical predictions for the mixture.

Fig. 3(a) shows an excellent match between the predictions of our model and the experimental data from Peng et al. (2007) for a gas mixture consisting of 73% CH_4 and 27% C_2H_4. Our model also predicts the film growth of pure ethylene hydrates very well using Eqs. (2.1), (2.2) and (2.13). A relevant plot including the match of the experimental data with our theory is included in the supplementary information (Fig S2(b)).

Fig. 3(b) shows a good match between our theoretical predictions of film growth and experiments for a mixture of 75% CH_4 and 25% CO_2. Experimental data was reported by Daniel-david et al. (2015), wherein they measured film growth on sessile droplets as an area velocity (mm^2/sec) at varying subcoolings. The reported data was normalized by a factor of twice the diameter to obtain the approximate linear velocity of film growth (for adapting to our model). The normalization factor was obtained by taking a ratio of the contour length of the droplet to its hemispherical area. Also, their experiments were not conducted at a constant temperature, but varied between 273 and 275 K. An average temperature of 274 K was utilized in our model.

5.3. Using higher order corrections for pure component hydrates

Finally, we report an interesting finding that higher order correlations like Eq. (2.13) can yield better predictions than those resulting from the use of Antoine formulation (Eq. (2.4)). It is noted that analytical closed-form solutions (like Eq. (2.9)) are not possible with the use of higher order correlations. Simulations were conducted to predict film velocities and the results were compared with experimental data from Peng et al. (2007) (detailed in Fig. 2a). In the supplementary material, we report a better match with experimental data with the use of the higher order correlations (R^2 > 0.99, as reported in Fig. S2 vs. R^2 = 0.98, as reported in Fig. 2a).

6. Perspectives on diffusion-based modeling of film growth

This section discusses various implications and aspects of the currently developed model. Firstly, while we analytically show that heat transfer is not the rate determining phenomena during short duration film growth on gas-water interfaces, there could be instances where heat transfer can influence film growth. Specifically, this would occur if the kinetics of hydrate formation was significantly accelerated through the use of promoters. The scaling analysis in Eqs. (1.2) and (1.4) suggests that if the rate of heat generation is accelerated by a factor of 100, the temperature in the vicinity of hydrate crystals would no longer be close to the temperature of the experiment. In such cases, temperature corrections would be needed in the temperature term in the denominator of the equilibrium concentration, c_{eq}, in Eq. (2.1). However, promoters like SDS (sodium dodecyl sulphate) often reduce the initial film thickness of hydrate formation (Kuang et al., 2018), which would lessen the magnitude of heat generation, even under faster formation kinetics. Our diffusion-based formulation could therefore conceivably explain film growth formation of gas hydrates in SDS solutions, which can be the subject of future studies.

Secondly, while this work focuses on gas-liquid interfaces, film formation of hydrates is also observed on liquid-liquid interfaces. Due to lack of experimental data on film formation on liquid-liquid interfaces, it is difficult to validate any related models. We believe that our diffusion-based formulation can also predict film growth on liquid-liquid interfaces; however, the concentrations have to be defined differently in Eq. (2.1). Commonly used liquids used to form clathrate hydrates are cyclopentane and tetrahydrofuran (THF). THF is miscible with water and will not exhibit film growth (Carpenter and Bahadur, 2016). Cyclopentane hydrates, however, do exhibit film growth; a slow temperature rise in the vicinity of the hydrate formation region has also been observed (Corak et al., 2011).

Thirdly, we note that while our model captures the fundamental aspects of hydrate film growth on a gas-water interface with one fitting parameter (which is the temperature-dependent overall rate constant K), we observe very narrow ranges of K for a particular set of experimental data. The detailed dependence of K on temperature and the hydrodynamic perturbations (as discussed earlier) is not currently explored. Hydrate experiments involve pressure vessels, which imposes stringent limitations on

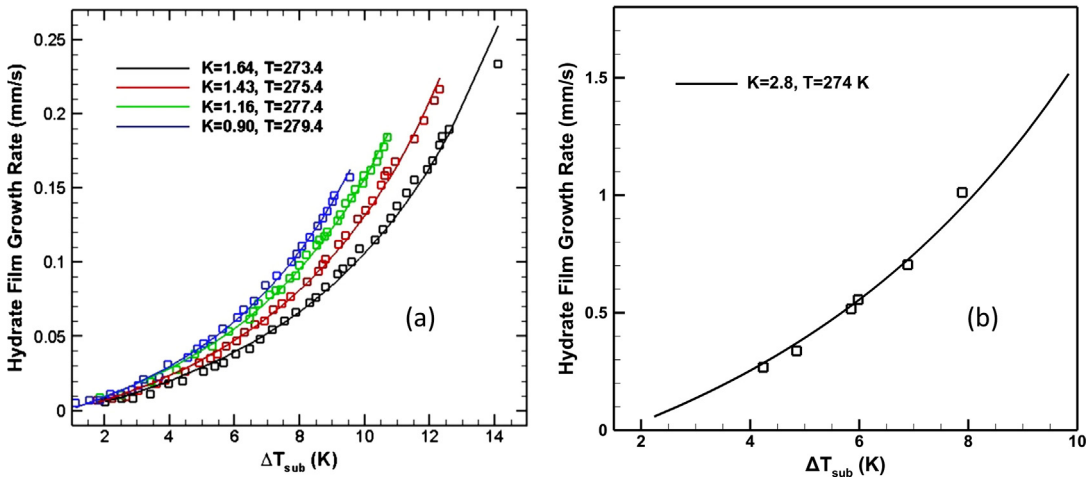

Fig. 3. Comparison of predictions of present model with experimentally measured growth rate of hydrate films formed from (a) mixture of 73% CH_4 and 27% C_2H_4 (Peng et al., 2007). (b) mixture of 75% CH_4 and 25% CO_2 (Daniel-david et al., 2015). The plot compares theoretical predictions (curves) to experimental data (squares). K is the fitting parameter with units of 10^{-4} m^4/mol sec for (a) and 10^{-3} m^4/mol sec for (b). All R^2 values are greater than 0.99.

instrumentation needed to accurately measure localized temperatures and film velocity. This makes it challenging to quantify the temperature sensitivity of K. Moreover, we believe that to better understand such aspects, the sharp interface-based modeling approach adopted in this literature would be insufficient, and diffuse interface considerations would be needed.

7. Conclusions

We report a diffusion-based analytical formulation to model film growth of hydrates, in contrast to previous models which utilize heat transfer considerations to explain film growth. Our model is applicable to any shape of the hydrate film front, unlike past models, and does not utilize the common assumption of film thickness being inversely proportional to subcooling. The model shows excellent agreement with multiple data sets reporting hydrate film growth from pure gases and mixtures of gases. In one case (Fig. 2d), our model is applicable over a much broader temperature/pressure range than a previous model based on heat transfer limitations. Overall, we believe that the science of film growth is better represented by a diffusion-limited kinetics rather than heat transfer-limited. We note that while this work suggests that film growth is diffusion-dominated, heat transfer will play a significant role in later stages of hydrate growth along with gas diffusion considerations through the hydrate layer.

CRediT authorship contribution statement

Aritra Kar: Conceptualization, Methodology, Investigation, Data curation, Formal analysis, Visualization, Writing - original draft. **Awan Bhati:** Methodology, Investigation, Formal analysis, Visualization. **Palash V. Acharya:** Methodology, Validation, Writing - review & editing. **Ashish Mhadeshwar:** Methodology, Validation, Writing - review & editing. **Pradeep Venkataraman:** Methodology, Validation, Writing - review & editing. **Timothy A. Barckholtz:** Methodology, Validation, Writing - review & editing. **Vaibhav Bahadur:** Methodology, Writing - review & editing, Supervision, Project administration.

Declaration of Competing Interest

The authors declare that they have no known competing financial interests or personal relationships that could have appeared to influence the work reported in this paper.

Acknowledgments

Research on CO_2 hydrates was supported by ExxonMobil through its membership in The University of Texas at Austin Energy Institute. This acknowledgment should not be considered an endorsement of the results by ExxonMobil. V.B. acknowledges NSF-CBET grant 1653412 for partial support of this work. P. V. Acharya acknowledges the support of the University Graduate Continuing Fellowship from UT Austin.

Appendix A. Supplementary material

Supplementary data to this article can be found online at https://doi.org/10.1016/j.ces.2021.116456.

References

Acharya, P.V., Kar, A., Shahriari, A., Bhati, A., Mhadeshwar, A., Bahadur, V., 2020. Aluminum-based promotion of nucleation of carbon dioxide hydrates. J. Phys. Chem. Lett. 1477–1482. https://doi.org/10.1021/acs.jpclett.9b03485.

Bahadori, A., Vuthaluru, H.B., 2009. A novel correlation for estimation of hydrate forming condition of natural gases. J. Nat. Gas Chem. 18, 453–457. https://doi.org/10.1016/S1003-9953(08)60143-7.

Buanes, T., Kvamme, B., Svandal, A., 2006. Computer simulation of CO_2 hydrate growth. J. Cryst. Growth 287, 491–494. https://doi.org/10.1016/j.jcrysgro.2005.11.074.

Carpenter, K., Bahadur, V., 2016. Electronucleation for rapid and controlled formation of hydrates. J. Phys. Chem. Lett. 7, 2465–2469. https://doi.org/10.1021/acs.jpclett.6b01166.

Corak, D., Barth, T., Høiland, S., Skodvin, T., Larsen, R., Skjetne, T., 2011. Effect of subcooling and amount of hydrate former on formation of cyclopentane hydrates in brine. Desalination 278, 268–274. https://doi.org/10.1016/j.desal.2011.05.035.

Daniel-david, D., Guerton, F., Dicharry, C., Torré, J., 2015. Hydrate growth at the interface between water and pure or mixed CO2 / CH4 gases: influence of pressure, temperature, gas composition and water-soluble surfactants. Chem. Eng. Sci. 132, 118–127. https://doi.org/10.1016/j.ces.2015.04.015.

Dashti, H., Thomas, D., Amiri, A., 2019. Modeling of hydrate-based CO_2 capture with nucleation stage and induction time prediction capability. Journal of Cleaner Production 231, 805–816.

Davies, M.E., Davies, R.J., 2003. Fundamentals of Chemical Reaction Engineering. McGraw-Hill, New York.

Davies, S.R., Sloan, E.D., Sum, A.K., Koh, C.A., 2010. In situ studies of the mass transfer mechanism across a methane hydrate film using high-resolution confocal Raman spectroscopy. J. Phys. Chem. C 114, 1173–1180. https://doi.org/10.1021/jp909416y.

Englezos, P., Kalogerakis, N., Dholabhai, P.D., Bishnoi, P.R., 1987. Kinetics of formation of methane and ethane gas hydrates. Chem. Eng. Sci. 42 (11), 2647–2658.

Freer, E.M., Sami Selim, M., Dendy Sloan, E., 2001. Methane hydrate film growth kinetics. Fluid Phase Equilib. 185, 65–75. https://doi.org/10.1016/S0378-3812(01)00457-5.

Fu, X., Cueto-Felgueroso, L., Juanes, R., 2018. Nonequilibrium thermodynamics of hydrate growth on a gas-liquid interface. Phys. Rev. Lett. 120, 144501. https://doi.org/10.1103/PhysRevLett.120.144501.

Hashemi, S., Macchi, A., Servio, P., 2007. Gas hydrate growth model in a semibatch stirred tank reactor. Ind. Eng. Chem. Res. 46, 5907–5912. https://doi.org/10.1021/ie061048.

Herri, J.M., Pic, J.S., Gruy, F., Cournil, M., 1999. Methane hydrate crystallization mechanism from in-situ particle sizing. AIChE J. 45, 590–602. https://doi.org/10.1002/aic.690450316.

Khurana, M., Yin, Z., Linga, P., 2017. A review of clathrate hydrate nucleation. ACS Sustain. Chem. Eng. 5, 11176–11203. https://doi.org/10.1021/acssuschemeng.7b03238.

Kishimoto, M., Ohmura, R., 2012. Correlation of the growth rate of the hydrate layer at a guest/liquid-water interface to mass transfer resistance. Energies 5, 92–100. https://doi.org/10.3390/en5010092.

Kitamura, M., Mori, Y.H., 2013. Clathrate-hydrate film growth along water/methane phase boundaries – an observational study. Cryst. Res. Technol. 48, 511–519. https://doi.org/10.1002/crat.201300095.

Koh, C.A., Sloan, E.D., Sum, A.K., Wu, D.T., 2011. Fundamentals and Applications of Gas Hydrates. https://doi.org/10.1146/annurev-chembioeng-061010-114152.

Kuang, Y., Lei, X., Yang, L., Zhao, Y., Zhao, J., 2018. Observation of in situ growth and decomposition of carbon dioxide hydrate at gas-water interfaces using magnetic resonance imaging. Energy Fuels 32, 6964–6969. https://doi.org/10.1021/acs.energyfuels.8b01034.

Kumar, A., Kushwaha, O.S., Rangsunvigit, P., Linga, P., Kumar, R., 2016. Effect of additives on formation and decomposition kinetics of methane clathrate hydrates: application in energy storage and transportation. Can. J. Chem. Eng. 94, 2160–2167. https://doi.org/10.1002/cjce.22583.

Lei, L., Seol, Y., Myshakin, E.M., 2019. Methane hydrate film thickening in porous media. Geophys. Res. Lett. 46, 11091–11099. https://doi.org/10.1029/2019GL084450.

Li-Li, S., Sun, C.Y., Liu, B., Feng, X.-J., Li, F.-G., 2013. Initial thickness measurements and insights into crystal growth of methane hydrate film. AIChE J. 59, 2145–2154. https://doi.org/10.1002/aic.13987.

Li, S., Sun, C., Liu, B., Li, Z., Chen, G., Sum, A.K., 2014. New observations and insights into the hydrate films. Scientific Rep. 4, 4129. https://doi.org/10.1038/srep04129.

Liu, Z., Li, H., Chen, L., Sun, B., 2018. A new model of and insight into hydrate film lateral growth along the gas-liquid interface considering natural convection heat transfer. Energy and Fuels 32, 2053–2063. https://doi.org/10.1021/acs.energyfuels.7b03530.

Makogon, Y., 1997. Hydrates of Hydrocarbons. PennWell Publishing Co..

Melhem, G.A., Saini, R., Goodwin, B.M., 1989. A modified Peng-Robinson equation of state. Fluid Phase Equilib. 47, 189–237. https://doi.org/10.1016/0378-3812(89)80176-1.

Mochizuki, T., Mori, Y.H., 2017. Simultaneous mass and heat transfer to/from the edge of a clathrate-hydrate film causing its growth along a water/guest-fluid phase boundary. Chem. Eng. Sci. 171, 61–75. https://doi.org/10.1016/j.ces.2017.05.015.

Mochizuki, T., Mori, Y.H., 2006. Clathrate-hydrate film growth along water/hydrate-former phase boundaries-numerical heat-transfer study. J. Cryst. Growth 290, 642–652. https://doi.org/10.1016/j.jcrysgro.2006.01.036.

Mori, Y.H., 2001. Estimating the thickness of hydrate films from their lateral growth rates: application of a simplified heat transfer model. J. Cryst. Growth 223, 206–212. https://doi.org/10.1016/S0022-0248(01)00614-5.

Morrissy, S.A., Mckenzie, A.J., Graham, B.F., Johns, M.L., May, E.F., Aman, Z.M., 2017. Reduction of clathrate hydrate film growth rate by naturally occurring surface active components. Energy Fuels. 31, 5798–5805. https://doi.org/10.1021/acs.energyfuels.6b02942.

Nellis, G., Klein, S., 2009. Heat Transfer. Cambridge University Press.

Peng, B.Z., Dandekar, A., Sun, C.Y., Luo, H., Ma, Q.L., Pang, W.X., Chen, G.J., 2007. Hydrate film growth on the surface of a gas bubble suspended in water. J. Phys. Chem. B. 111, 12485–12493. https://doi.org/10.1021/jp074606m.

Ribeiro, C.P., Lage, P.L.C., 2008. Modelling of hydrate formation kinetics: State-of-the-art and future directions. Chem. Eng. Sci. 63, 2007–2034. https://doi.org/10.1016/j.ces.2008.01.014.

Saito, K., Sum, A.K., Ohmura, R., 2010. Correlation of hydrate-film growth rate at the guest/liquid-water interface to mass transfer resistance. Ind. Eng. Chem. Res. 49, 7102–7103. https://doi.org/10.1021/ie1000696.

Sloan, E.D., Koh, C.A., 2008. Clathrates Hydrates of the Natural Gases.

Sugaya, M., Mori, Y.H., 1996. Behaviour of clathrate hydrate formation at the boundary of liquid water and a fluorocarbon in liquid or vapor state. Chemical Engineering Science 51 (13), 3505–3517.

Sun, C.Y., Chen, G.J., Ma, C.F., Huang, Q., Luo, H., Li, Q.P., 2007. The growth kinetics of hydrate film on the surface of gas bubble suspended in water or aqueous surfactant solution. J. Cryst. Growth 306, 491–499. https://doi.org/10.1016/j.jcrysgro.2007.05.037.

Sun, C.Y., Peng, B.Z., Dandekar, A., Ma, Q.L., Chen, G.J., 2010. Studies on hydrate film growth. Annu. Rep. Prog. Chem. Sect. C 106, 77–100. https://doi.org/10.1039/b811053k.

Taylor, C.J., Miller, K.T., Koh, C.A., Sloan, E.D., 2007. Macroscopic investigation of hydrate film growth at the hydrocarbon/water interface. Chem. Eng. Sci. 62, 6524–6533. https://doi.org/10.1016/j.ces.2007.07.038.

Turner, D.J., Miller, K.T., Dendy Sloan, E., 2009. Methane hydrate formation and an inward growing shell model in water-in-oil dispersions. Chem. Eng. Sci. 64, 3996–4004. https://doi.org/10.1016/j.ces.2009.05.051.

Uchida, T., Ebinuma, T., Kawabata, J., Narita, H., 1999. Microscopic observations of formation processes of clathrate-hydrate films at an interface between water and carbon dioxide. J. Cryst. Growth 204, 348–356. https://doi.org/10.1016/S0022-0248(99)00178-5.

Vlasov, V.A., 2013. Formation and dissociation of gas hydrate in terms of chemical kinetics. React. Kinet. Mech. Catal. 110, 5–13. https://doi.org/10.1007/s11144-013-0578-x.

Wu, R., Kozielski, K.A., Hartley, P.G., May, E.F., Boxall, J., Maeda, N., 2013. Methane – propane mixed gas hydrate film growth on the surface of water and luvicap EG solutions. Energy Fuels 27, 2548–2554. https://doi.org/10.1021/ef4003268.

Yin, Z., Khurana, M., Tan, H.K., Linga, P., 2018. A review of gas hydrate growth kinetic models. Chem. Eng. J. 342, 9–29. https://doi.org/10.1016/j.cej.2018.01.120.